VEHICLE SPEED AND SPACING CONTROL VIA COORDINATED THROTTLE AND BRAKE ACTUATION

J. Christian Gerdes J. Karl Hedrick

Department of Mechanical Engineering
University of California
Berkeley, CA

Abstract. This paper presents a combined engine and brake controller for automated highway vehicles incorporating the ideas of multiple-surface sliding control. The controller consists of three elements: a task-dependent "upper" sliding controller that incorporates vehicle acceleration as a synthetic input, a switching logic that chooses between brake or throttle control and individual "lower" sliding controllers for the brake and engine dynamics. In particular, the introduction of the brake control scheme and switching logic represent a substantial improvement over previous work. Experimental results show that the closed-loop system is capable of tracking velocity profiles within 0.1 m/s and following a maneuvering lead car at a distance of 2 meters with only 20 centimeter error.

Keywords. Automotive Control, Brakes, IVHS, Nonlinear Control, Sliding Surfaces.

1. INTRODUCTION

With traffic density continuing to increase, the idea of using highway automation to increase capacity is growing steadily more attractive. Whether the system envisioned involves an intelligent cruise control capable of speed tracking and vehicle following (Ioannou and Xu, 1994) or coordinated "platoons" of closely-spaced vehicles (McMahon *et al.*, 1990), however, successful implementation hinges on the ability to accurately control vehicle dynamics. Since these dynamics are highly nonlinear and uncertain, this is no small task.

For these reasons, McMahon *et al.* (1990) introduced the idea of a multiple-surface sliding controller structure for vehicle following. This paper expands upon that idea to produce a coordinated engine and brake controller capable of performing all of the (non-emergency) longitudinal control tasks required on an automated highway. The resulting structure consists of an upper sliding controller defined by the specific control task, a switching logic to determine whether engine or brake control is required and separate sliding controllers capable of tracking the desired engine and brake torques.

Section 2 presents the single-state longitudinal model which serves as both a state equation and a means of determining the required brake or engine torque. The following two sections present sliding controllers based upon the nonlinear brake dynamic model of Gerdes *et al.* (1995) and the engine model of Cho and Hedrick (1989). Section 5 details the upper surface development for both speed and spacing control and adapts a switching logic proposed by Gerdes and Hedrick (1995) to coordinate the throttle and brake commands. The paper concludes with experimental results demonstrating that the closed-loop system is capable of tracking velocity profiles within 0.1 m/s and following a maneuvering lead car at a distance of 2 meters with only 20 centimeter error.

2. LONGITUDINAL VEHICLE MODEL

Assuming that no slip occurs either at the tire-road interface or across the vehicle's torque converter (a reasonable assumption for gradual maneuvers at highway speeds, McMahon *et al.* (1990)), vehicle speed, v, and engine speed, ω_e are related by:

$$v = R_g \, h \, \omega_e \tag{1}$$

where R_g is the gear ratio and h the tire radius. The longitudinal state equation can then be written by reflecting all of the forces and torques on the vehicle to the engine, yielding:

$$\dot{v} = \frac{1}{\beta}[\tau_e - R_g \, (\tau_b + M_{rr} + hF_a + mgh \sin\theta)] \tag{2}$$

where β is the lumped inertia, M_{rr} is the rolling resistance, F_a is an aerodynamic drag force of the form $F_a = C_a v^2$, θ is the road grade and τ_e and τ_b denote the engine and brake torques.

Equation 2 may be viewed both as a state equation for v and as a means for determining the necessary brake or engine torque required to produce a given acceleration. In this latter context, the control problem becomes a matter of determining the desired acceleration, calculating the engine or brake torque necessary and tracking these torques with individual controllers.

3. BRAKE CONTROL

To overcome the limitations imposed by the brake vacuum booster (Gerdes and Hedrick, 1995), the brake system used in this study incorporates a separate actuator mounted between the booster and the master cylinder (Figure 1). Since this actuator is sufficiently fast, the master cylinder pressure, P_{mc}, becomes the input to the brake system and the total brake torque developed can be determined from the single-state model by Gerdes *et al.* (1995). In this model, the brake torque is proportional to the pressure at the wheel, P_w, through gain K_b after a small "push-out" pressure, P_{po}:

$$\tau_b = \begin{cases} K_b(P_w - P_{po}) & P_w > P_{po} \\ 0 & \text{otherwise} \end{cases} \tag{3}$$

The wheel pressure is considered a function of the displaced brake fluid, V, as shown in Figure 2, and the fluid dynamics are described by:

$$\dot{V} = \sigma C_q \sqrt{|P_{mc} - P_w|} \tag{4}$$

where C_q is a flow coefficient and $\sigma = sgn(P_{mc} - P_w)$.

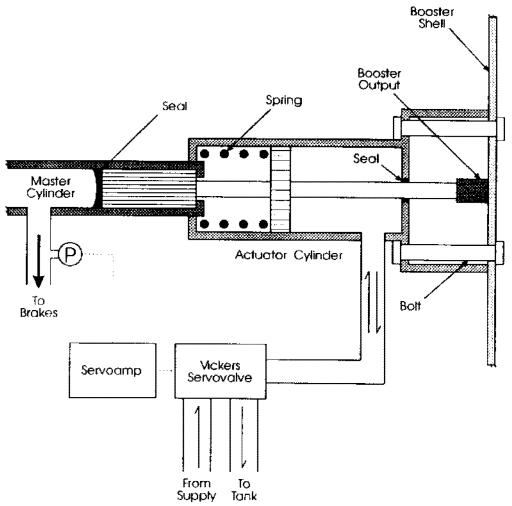

Fig. 1. Direct Master Cylinder Actuation System

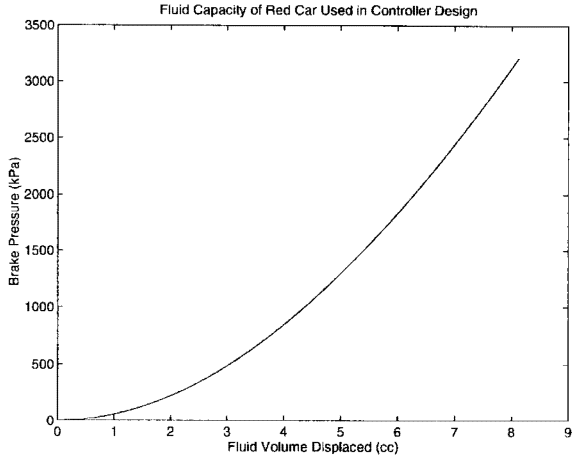

Fig. 2. Brake Fluid Capacity Curve

During general maneuvers in a platoon, the brake pressures required are generally rather small; hence the flow rate, $\dot{V}$, resulting from an open loop command is also quite small. Because of the nature of the fluid capacity curve in Figure 2, the system therefore exhibits long delays between the time the brake pressure is commanded and the time it appears at the wheel. Since such delays lead to performance constraints on the automated vehicle, as noted by Gerdes and Hedrick (1995), some form of lead compensation is required.

Because measurement of wheel torque is prohibitively expensive, feedback for this compensation comes from the wheel pressure. The plant dynamics therefore describe a first-order, nonlinear system, suggesting a simple sliding control approach. Translating τ_{bdes} into a desired wheel pressure, P_{wdes}, set

$$S_b = P_{wdes} - P_w \tag{5}$$

$$\dot{S}_b = -\lambda_b S_b \tag{6}$$

Substituting the actual dynamics yields

$$\dot{P}_w = \dot{P}_{wdes} - \lambda_b S_b \tag{7}$$

where

$$\dot{P}_w = \frac{\partial P_w}{\partial V} \sigma C_q \sqrt{|P_{mc} - P_w|} \tag{8}$$

If Equation 8 were well-defined everywhere, it could be used in conjunction with Equation 7 to determine the desired value of the control input, P_{mc}. Unfortunately, because of the nature of the wheel capacitance in Figure 2, $\frac{\partial P_w}{\partial V}$ is not defined until the initial flow to the caliper occurs.

This may be remedied by defining a lower limit on $\frac{\partial P_w}{\partial V}$ in the controller to be a and the pressure and volume at which $\frac{\partial P_w}{\partial V} = a$ to be P_a and V_a. Then the master cylinder pressure commanded can be given by:

$$\dot{P}_{wdes} > \lambda_b (P_w - P_{wdes}) \Longrightarrow$$

$$P_{mc} = P_w + \left(\frac{\dot{P}_{wdes} - \lambda_b (P_w - P_{wdes})}{\frac{\delta P_w}{\delta V} C_q} \right)^2 \tag{9}$$

$$\dot{P}_{wdes} < \lambda_b (P_w - P_{wdes}) \Longrightarrow$$

$$P_{mc} = P_w - \left(\frac{\dot{P}_{wdes} - \lambda_b (P_w - P_{wdes})}{\frac{\delta P_w}{\delta V} C_q} \right)^2 \tag{10}$$

where

$$\frac{\delta P_w}{\delta V} = \begin{cases} \frac{\partial P_w}{\partial V} & P_w > P_a \\ a & \text{otherwise} \end{cases} \tag{11}$$

Note that since P_w provides the feedback, this involves writing $\frac{\delta P_w}{\delta V}$ as a function of P_w and not V (which is possible since $P_w(V)$ is invertible above V_a). In practice, P_a can be chosen to be below the pushout pressure, P_{po}, at which braking commences. Loosely speaking, therefore, only pressures above P_a are of interest and the controller functions as a sliding controller above P_a. It can furthermore be shown that for trajectories satisfying $P_{wdes}(t) > P_{po}$, the controller begins to function as a sliding controller in a finite time (Gerdes, 1996).

4. ENGINE CONTROL

The engine model is based upon the two-state model of Cho and Hedrick (1989), which was previously used for longitudinal control by McMahon *et al.* (1990), Choi and Devlin (1995) and Gerdes and Hedrick (1995). In this model, the engine torque production is continuous and determined from a steady-state engine map

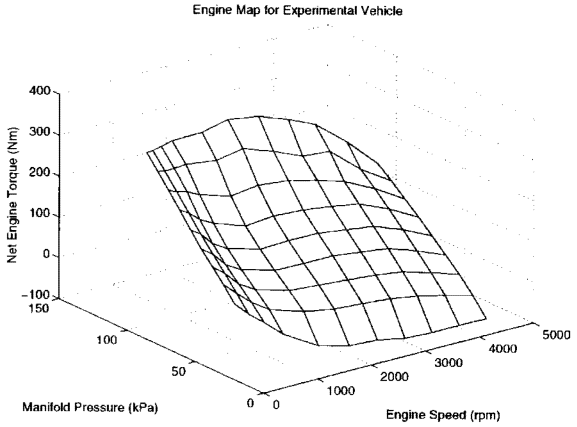

Fig. 3. Engine Map for Experimental Vehicle

$$\tau_e = \tau_e (\omega_e, P_m) \tag{12}$$

where P_m is the pressure in the engine intake manifold. Figure 3 shows this map for one of the experimental vehicles, based upon data from the manufacturer.

The two states are taken to be the engine speed, ω_e, and the mass of air in the intake manifold, m_a (assuming the ideal gas law holds, $P_m V_m = m_a RT$, so the manifold pressure and air mass may be used interchangeably). The state equation for ω_e is simply Equation 2, while the state equation for m_a is given by continuity:

$$\dot{m}_a = \dot{m}_{ai} - \dot{m}_{ao} \tag{13}$$

The mass of air flowing into the intake manifold is:

$$\dot{m}_{ai} = \text{MAX TC}(\alpha)\,\text{PRI}(m_a) \tag{14}$$

where MAX represents the flow rate at full throttle, α is the throttle angle, $\text{TC}(\alpha)$ is an empirical throttle characteristic and $\text{PRI}(m_a)$ a pressure influence function for compressible flow:

$$\text{PRI} = 1 - \exp\left(9 \cdot \left(\frac{P_m}{P_{atm}} - 1\right)\right) \tag{15}$$

The mass of air flowing out of the intake manifold and into the cylinders, $\dot{m}_{ao}$, is determined from tables provided by the manufacturer.

When the throttle is completely closed, the throttle characteristic is zero, but air continues to flow into the manifold through the throttle bypass. The effect of the bypass is to create a minimum manifold pressure which varies according to engine speed (see Figure 4) and serves to

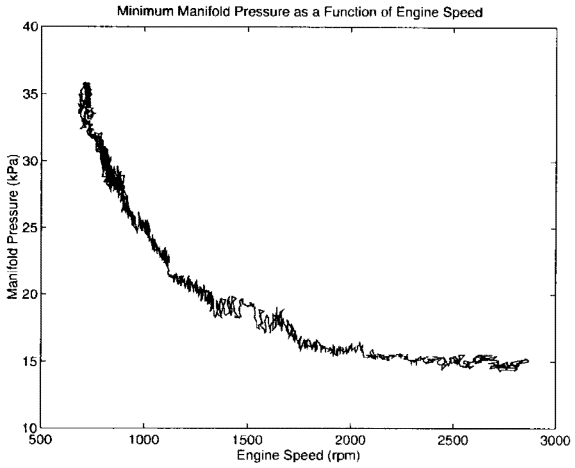

Fig. 4. Closed Throttle Engine Behavior

define the lower edge of the map in Figure 3. Physically, the manifold pressure decays to this surface in the absence of any throttle input and remains there until the throttle is again opened.

The controller used for the engine (McMahon *et al.*, 1990) calculates the desired value of the throttle angle, α, so that the engine net torque production, τ_e, tracks the desired value, τ_{edes}. Using the principle that the dynamics associated with the mass of air in the intake manifold (Equation 13) are much faster than those associated with the engine speed (Equation 2), τ_{edes} can be translated into a desired value of m_a at the current value of ω_e by solving Equation 12 implicitly:

$$\tau_{edes} = \tau_e\left(\omega_e, P_{mdes}\right) \tag{16}$$

Transforming P_{mdes} to m_{ades}, the sliding controller for the engine is given by:

$$S_e = m_a - m_{ades} \tag{17}$$

$$\dot{S}_e = -\lambda_e S_e \tag{18}$$

Using Equations 13 through 15, the sliding surface equations yield a desired flow of air into the manifold:

$$\dot{m}_{ai} = \dot{m}_{ao} + \dot{m}_{ades} - \lambda_e\left(m_a - m_{a,des}\right) \tag{19}$$

From this, follows the desired throttle characteristic:

$$TC\left(\alpha\right) = \left(\dot{m}_{ao} + \dot{m}_{ades} - \lambda_e S_e\right) / \left(\text{MAX PRI}\right) \tag{20}$$

Inverting the desired value of the throttle characteristic yields the value of the control, α.

5. SPEED AND SPACING CONTROL

From a design standpoint, it is highly desirable to decouple the engine and brake control tasks from the overall vehicle control task (e.g. speed tracking or following). Such decoupling allows the same control task to be performed on any vehicle, thereby freeing the highway designer from considering nuances of engine and brake dynamics on individual vehicles. Since an automated highway will no doubt contain vehicles of various of various manufacture, modularity in this fashion provides a very realistic approach.

This goal may be accomplished by creating separate "upper" sliding controllers for each task which treat the vehicle acceleration as a synthetic input. The switching logic in Section 5.3 may then be used to determine the engine or brake torque necessary to achieve this acceleration and the throttle or brake controllers of the previous sections subsequently employed to track the desired torques. The following sections illustrate how this procedure may be employed to create a controller capable of speed tracking or following. The additional longitudinal actions of platoon joining and splitting may be handled similarly (Connolly and Hedrick, 1996).

5.1 *Speed Control*

The sliding controller for speed tracking is fairly trivial. Given a desired velocity, $v_{des}(t)$, define the sliding surface S_u by:

$$S_u = v - v_{des} \tag{21}$$

Clearly, the control objective is satisfied when $S_u = 0$. To achieve this, the system state is "driven" to this surface by defining

$$\dot{S}_u = -\lambda_u S_u \tag{22}$$

Solving Equation 22 yields the desired acceleration:

$$a_{des} = \dot{v}_{des} - \lambda_u\left(v - v_{des}\right) \tag{23}$$

5.2 *Spacing Control*

Several formulations of spacing control or vehicle follower laws have appeared in the literature. The one presented here is a simple version of the control law of McMahon *et al.* (1990) for the case of two cars. Denoting the position, velocity and acceleration of the lead car by x_l, $\dot{x}_l$ and $\ddot{x}_l$, and the corresponding quantities

for the follower by x, $\dot{x}$ and $\ddot{x}$, define the spacing error, ϵ, by:

$$\epsilon = \Delta - (x_l - x) \tag{24}$$

where Δ is the (constant) desired spacing. Placing the pole for the spacing error dynamics at K_ϵ, set

$$S_u = \dot{\epsilon} + K_\epsilon \epsilon \tag{25}$$

As with the speed control task above, the objective is satisfied when $S_u = 0$, so setting $\dot{S}_u = -\lambda_u S_u$ yields:

$$a_{des} = \ddot{x}_l - K_\epsilon \dot{\epsilon} - \lambda_u S_u \tag{26}$$

5.3 *Switching Between Throttle and Brakes*

Section 4 described the behavior of the engine when the throttle angle is set to zero and illustrated how the closed-throttle behavior defines the lower edge of the engine map. While Figure 4 projected this edge into the $\omega_e - P_{man}$ plane, this curve also determines a minimum torque, described by the projection into the $\omega_e - \tau_e$ plane. This brings to light a certain distinction between the engine and brake torques in vehicle motion; namely, that some engine torque is always produced. As a result, the engine torque can be divided into two parts: the minimum (closed-throttle) torque, τ_{et}, and the portion subject to control, τ_{ec} (which represents the height above the lower edge in the engine map of Figure 3).

Physically, a desired acceleration greater than the acceleration of the vehicle due to the drag forces and τ_{et} requires a positive throttle angle; acceleration less than this requires braking. Thus a natural switching condition between brake and throttle control can be found in the physics of the problem. Graphically, this condition may be viewed as a function of desired acceleration and the current vehicle speed, as demonstrated in Figure 5, which shows the switching criterion for the experimental vehicle in 3rd gear. As the dotted lines suggest, a small hysteresis can easily be included in this condition to eliminate chatter.

In terms of equations, the condition is:

$$\beta a_{des} + R_g \left(M_{rr} + F_a + mg \sin\theta\right) - \tau_{et} \geq 0$$
$$\Longrightarrow \text{Throttle Control} \tag{27}$$

$$\beta a_{des} + R_g \left(M_{rr} + F_a + mg \sin\theta\right) - \tau_{et} < 0$$
$$\Longrightarrow \text{Brake Control} \tag{28}$$

For throttle control, the desired torque is:

$$\tau_{edes} = \beta a_{des} + R_g \left(M_{rr} + hF_a + mgh \sin\theta\right) \tag{29}$$

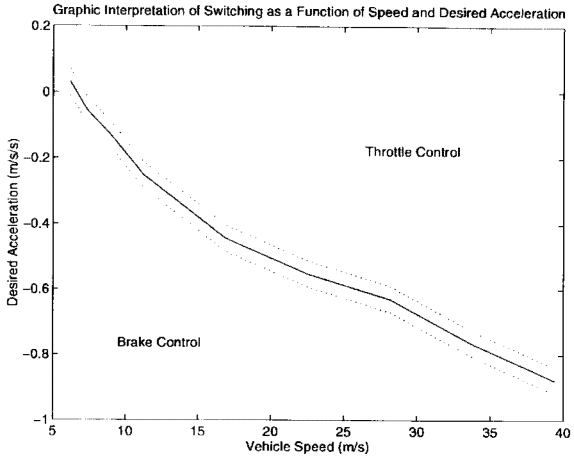

Fig. 5. Switching Condition for 3rd Gear Operation

and for brake control, the desired torque is:

$$\tau_{bdes} = -\frac{(\beta a_{des} + \tau_{et})}{R_g} - M_{rr} - hF_a - mgh \sin\theta \tag{30}$$

Since this switching rule depends only upon one of the vehicle states (namely, v) and the desired acceleration, it is independent of the specific upper surface controller chosen. Hence, this switching condition is suitable for use with any vehicle control objective, as opposed to being task-specific (e.g. Ioannou and Xu (1994)). Furthermore, this switching condition avoids the high-frequency oscillation and risk of competing control inputs (Gerdes and Hedrick, 1995) that can occur with switches based upon the desired throttle angle (e.g. McMahon *et al.* (1990),Choi and Devlin (1995)). Finally, this method is much more amenable to analysis; indeed, a rigorous proof of stability (with respect to a set) for the system with hysteresis can be found in (Gerdes, 1996).

6. RESULTS

Due to space limitations, only experimental results are presented here; simulations of the controller may be found in Gerdes (1996). Figures 6 and 7 alone, however, provide a very strong testimony to the feasibility of the control structure. In the speed tracking experiment of Figure 6, the measured values of the manifold and brake pressures are barely distinguishable from the desired (dashed) values. Consequently, the speed tracking is excellent, with errors of only 0.1 m/s. Furthermore, the switching condition results in a very smooth transition between throttle and brake control.

Figure 7 shows a second vehicle following the first through this same maneuver. While the addition of the lead car

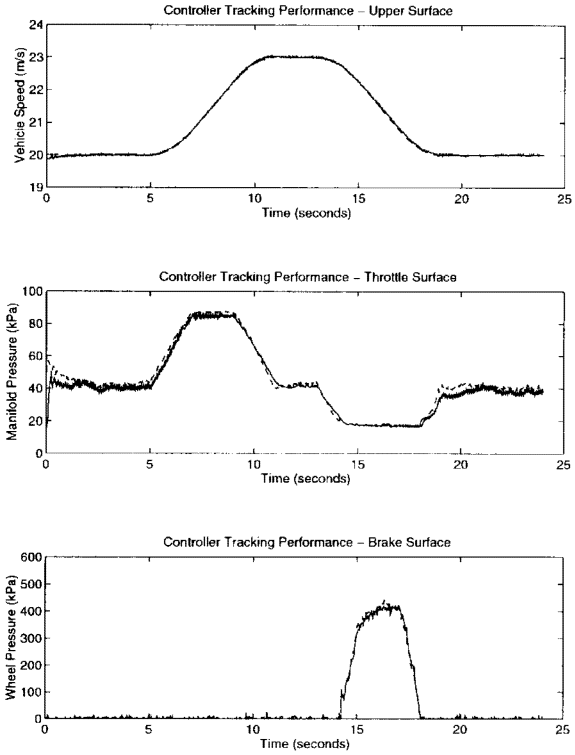

Fig. 6. Speed Tracking (Experimental)

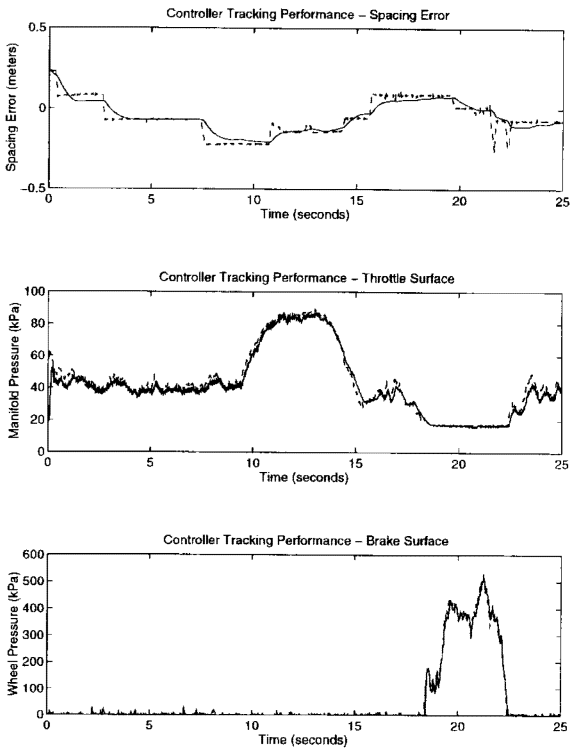

Fig. 7. Vehicle Following (Experimental)

acceleration to the control law adds some volatility to the desired engine and brake torques, tracking is still impressive. Indeed, the spacing error of approximately 20 cm is very close to the 15 cm discretization of the radar measurement (as can be seen by the comparison of raw and Kalman filtered radar signals in the top plot). The fact that spacings as close as 2 meters were successfully maintained without any passenger discomfort further underscores the success of the control structure.

7. ACKNOWLEDGEMENTS

The authors would like to thank Mr. Peter Devlin of the California PATH Program for developing the brake actuator cylinder and hydraulic supply and Mr. Fred Phillips and Mr. Jim Bloomquist of Vickers for donating the servovalve and electronics. This research was performed as a part of the PATH program at the University of California, in cooperation with the State of California, Business, Transportation, and Housing Agency, Department of Transportation, and the United States Department of Transportation, Federal Highway Administration. This work was supported in part by a National Science Foundation Graduate Research Fellowship.

8. REFERENCES

Cho, D. and J. K. Hedrick (1989). Automotive powertrain modeling for control. *ASME J. Dyn. Sys. Meas. Ctrl.* **111**, 568–576.

Choi, S. B. and P. Devlin (1995). Throttle and brake combined control for intelligent vehicle highway systems. SAE Paper # 951897.

Connolly, T. R. and J. K. Hedrick (1996). Longitudinal transition maneuvers in an automated highway system. Submitted to 1996 ASME IMECE.

Gerdes, J. C. (1996). PhD thesis. University of California at Berkeley.

Gerdes, J. C., A. S. Brown and J. K. Hedrick (1995). Brake system modeling for vehicle control. In: *Advanced Automotive Technologies - 1995 ASME IMECE.* pp. 105–112.

Gerdes, J. C. and J. K. Hedrick (1995). Brake system requirements for platooning on an automated highway. In: *Proc. 1995 ACC, Seattle, WA.* pp. 165–169.

Ioannou, P. and Z. Xu (1994). Throttle and brake control systems for automatic vehicle following. *IVHS Journal* **1**(4), 345–377.

McMahon, D. H., J. K. Hedrick and S. E. Shladover (1990). Vehicle modelling and control for automated highway systems. In: *Proc. 1990 ACC, San Diego, CA.* pp. 297–303.